academicJournals

Vol. 11(8), pp. 96-103, 30 April, 2016
DOI: 10.5897/IJPS2016.4460
Article Number: 1763BDD58284
ISSN 1992 - 1950

http://www.academicjournals.org/IJPS

International Journal of Physical Sciences

Full Length Research Paper

Slip flow of a second grade fluid past a lubricated rotating disc

K. Mahmood*, M. Sajid, N. Ali and T. Javed

Department of Mathematics and Statistics, International Islamic University, Islamabad 44000, Pakistan.

Received 1 January, 2016; Accepted 31 March, 2016

Slip flow of a second-grade fluid past a lubricated rotating disc is studied. The disc is lubricated with a power-law fluid. The interfacial conditions between fluid and lubricant are imposed on the surface of disc by assuming a thin lubrication layer. The numerical solutions are obtained using Keller-Box method. The effects of slip parameter and Weissenberg number on the three components of fluid velocity and pressure are analyzed graphically while effects on both components of skin friction are demonstrated through tables. The computed results show that spin-up by a second grade bulk fluid near the rotating disc is reduced by increasing slip at the interface. The obtained solutions agree well in the special case with those of other researches.

Key words: Non-Newtonian power-law fluid, second grade fluid, rotating disc, slip boundary condition.

INTRODUCTION

Technical applications of the flow over a rotating surface occur in many engineering and industrial fields. Some direct applications of flow over a rotating disc are waste water treatment, turbo-machinery, viscometry, centrifugal pumps, computer discs, sports discs, and rotating blades. The stagnation point flow of Newtonian fluid over a rotating disc was initially discussed by Von Karman (1921), who transformed the set of partial differential equations into ordinary differential equations by introducing an elegant similarity transformation and solved the resulting equations by momentum integral method. Due to the importance of rotating flows in the fields of engineering and technology, much extensions and modifications with more accurate solutions of Von Karman's flow have been presented in the literature. Cochran (1934) obtained asymptotic solution of the Von Karman's flow broblem. Benton (1966) improved the Cochran's results and extended the problem by taking into account the unsteady case. Sparrow and Gregg (1960) studied the steady state heat transfer from a rotating disc by taking different values of Prandtl numbers. Kakutani (1962), Sparrow and Chess (1962), Pande (1971), Watson and Wang (1979), Kumar et al. (1988) and Watanabe and Oyama (1991) discussed different aspects of electrically conducting viscous fluid over a rotating disc with heat transfer. Turkyilmazoglu (2015) analyzed Bödewadt flow and heat transfer over a stretching disk. Asghar et al. (2014) carried out Lie group

*Corresponding author. E-mail: khalidmeh2012@gmail.com.

analysis of flow and heat transfer of a viscous fluid on a rotating disk stretching in radial direction. In recent years, Turkyilmazoglu (2014); Turkyilmazoglu and Senel, (2013); Turkyilmazoglu, (2012a; b); Turkyilmazoglu, (2009) investigated different aspects of fluid flow and heat transfer due to rotating disc. Effects of slip at permeable disc are investigated by Miklavcic and Wang (2004). Hannah (1947) discussed the axisymmetric stagnation point flow of a viscous fluid towards a rotating disc for the first time. Tifford and Chu (1952) found the exact solution of the problem considered by Hannah (1947). Wang (2008) studied stagnation-point flow over an off-centered rotating disc and proved that non alignment complicates the flow problem. Asghar et al. (2007) investigated MHD flow due to non-coaxial rotation of an accelerated disc. Attia (2009) studied the flow due to a rotating disc under the influence of an external uniform magnetic field. In 2003, Wang (2003) investigated the stagnation point flow for a flat plate in the presence of slip boundary condition. The slip flow over a lubricated rotating disc was first considered by Andersson and Rousselet (2006). The axisymmetric stagnation point flow of a viscous fluid on a surface lubricated with a power-law fluid has been carried out by Santra et al. (2007).

In all the aforementioned studies, constitutive relationship of a viscous fluid is considered. However, fluids used in industry and technology do not obey Newton's law of viscosity and are called non-Newtonian fluids. For example, polymer solutions and melts, oil, paints, blood, etc., for which Navier-Stokes equations are inadequate. A number of non-Newtonian models have been proposed to predict the phenomena like normal stress effects, shear thinning, shear thickening, stress relaxation and retardation, etc. Amongst these non-Newtonian fluids, the second grade fluid is one that has been studied extensively. The equation of motion for second grade fluid is highly non-linear and one order higher than the Navier-Stokes equations. Therefore, to obtain a well posed problem, one requires additional boundary conditions to study the flow problems. Rajagopal and Gupta (1984) showed that to obtain a unique solution for the flow of a second-grade fluid in bounded geometry, an additional boundary condition is required. To overcome the requirement of additional boundary conditions, Beard and Walters (1964) discussed the stagnation point flow of a viscoelastic fluid by using a regular perturbation technique in which the perturbation parameter is the coefficient of the highest derivative. Garg and Rajagopal (1990) and Ariel (2002) augmented the boundary conditions at infinity in order to overcome this difficulty. In another investigation, Ariel (1997) studied the steady laminar flow of a second grade fluid near a rotating disc. Labropulu and Li (2008) discussed stagnation point flow of a second grade fluid with slip. MHD mixed convection in a vertical annulus filled with Al_2O_3-water nano-fluid considering nanoparticles migration was analyzed by Malvandi et al. (2015). Recently Afrand et al. (2015) discussed effects of magnetic field on free convection flow in inclined cylindrical annulus containing molten Potassium. Safaei et al. (2011) investigated numerical study of laminar mixed convection heat transfer of power-law non-Newtonian fluids in square enclosures by Finite Volume Method. A literature survey reveals that there is no attempt available for studying the slip flow of a second grade fluid over a lubricated rotating disc. The slip boundary condition at the interface between the second grade and power-law fluids is developed and numerical results are computed to discuss the behaviour of second grade fluid over a lubricated disk. The obtained results for a second grade fluid show a significant deviation from the available results for Newtonian fluid. The results for no-slip case are deduced as the special case from the obtained solutions. An implicit finite difference scheme known as Keller-Box method (Keller and Cebeci, 1972; Bradshaw et al., 1981; Keller, 1970) is employed to obtain the similarity solution.

MATHEMATICAL FORMULATION

Consider the steady, axisymmetric flow of a second grade fluid over a rotating disc lubricated with a thin layer of power law fluid. The flow rate Q of the lubricant is given by

$$Q = \int_0^{\delta(r)} U(r,z)\ 2\pi r dz\ , \tag{1}$$

where $U(r,z)$ is the radial component of the velocity vector of power-law fluid and $\delta(r)$ is the variable thickness of the lubrication layer. Moreover, disc is rotating with a uniform velocity ω about z-axis which is normal to the disc and the origin O is located at the center of the disc (Figure 1).

In the presence of these assumptions, the flow of a second grade fluid is governed by the following equations:

$$\nabla . \mathbf{v} = 0\ , \tag{2}$$

$$\rho(\mathbf{v}.\nabla\mathbf{v}) = -\nabla P + \mu\nabla^2\mathbf{v} - k_0\{\nabla^2(\mathbf{v}.\nabla)\mathbf{v} - 2(\mathbf{v}.\nabla)\nabla^2\mathbf{v}\}\ , \tag{3}$$

where $P(r,z)$ is the fluid pressure, ρ is density, μ is viscosity and k_0 is the second grade fluid parameter. The boundary condition at the surface is

$$U(r,0) = 0,\ \ V(r,0) = \omega r,\ \ W(r,0) = 0,\ \ P(r,0) = 0. \tag{4}$$

with

$$W(r,z) = 0\ ,\ \ \forall\ z \in [0,\delta(r)]. \tag{5}$$

The continuity of the shear stress at the interface $z = \delta(r)$ for both the fluids suggests:

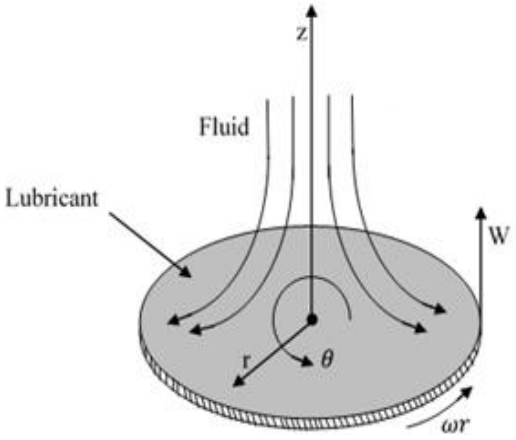

Figure 1. Diagram showing considered flow problem.

$$\mu\left(\frac{\partial u}{\partial z}\right)+k_0\left(\begin{array}{c}-\frac{v}{r}\frac{\partial v}{\partial z}-\frac{\partial u}{\partial z}\frac{\partial w}{\partial z}+\frac{\partial u}{\partial z}\frac{\partial u}{\partial r}+\frac{\partial v}{\partial z}\frac{\partial v}{\partial r}+\frac{\partial w}{\partial z}\frac{\partial w}{\partial r}-\frac{\partial u}{\partial r}\frac{\partial w}{\partial r}\\ +u\frac{\partial^2 u}{\partial r\partial z}+w\frac{\partial^2 u}{\partial z^2}+w\frac{\partial^2 w}{\partial r\partial z}+u\frac{\partial^2 w}{\partial r^2}\end{array}\right)=\mu_L\frac{\partial U}{\partial z}, \quad (6)$$

$$\mu\left(\frac{\partial v}{\partial z}\right)+k_0\left(\frac{u}{r}\frac{\partial v}{\partial z}-\frac{\partial v}{\partial z}\frac{\partial w}{\partial z}+w\frac{\partial^2 v}{\partial z^2}+\frac{v}{r}\frac{\partial w}{\partial r}-\frac{\partial v}{\partial r}\frac{\partial w}{\partial r}+u\frac{\partial^2 v}{\partial r\partial z}\right)=\mu_L\frac{\partial V}{\partial z}. \quad (7)$$

In Equations 6 and 7, μ_L is the viscosity of the power law fluid. Assuming

$\frac{\partial U}{\partial r}\ll\frac{\partial U}{\partial z}$ and $\frac{\partial V}{\partial r}\ll\frac{\partial V}{\partial z}$, μ_L can be written as

$$\mu_L=k\left[\left(\frac{\partial U}{\partial z}\right)^2+\left(\frac{\partial V}{\partial z}\right)^2\right]^{\frac{n-1}{2}}, \quad (8)$$

where *k* is the consistency coefficient and *n* is the flow behavior index of the power-law fluid. Assuming the linear variations of the radial and circumferential velocity components of power-law fluid inside the lubrication layer, we get

$$U(r,z)=\frac{\tilde{U}(r)\,z}{\delta(r)}, \quad (9)$$

$$V(r,z)=\omega r-\frac{(\omega r-\tilde{V}(r))\,z}{\delta(r)}. \quad (10)$$

Here $\tilde{U}(r)$ and $\tilde{V}(r)$ are interfacial velocity components of bulk second grade fluid and power law fluid. Thickness of the lubrication layer can be evaluated by substituting Equation 9 into Equation 1:

$$\delta(r)=\frac{Q}{\pi\, r\tilde{U}(r)}. \quad (11)$$

Since at the interface

$$\tilde{U}=u\,,\ \tilde{V}=v \quad (12)$$

Therefore, Equations 6 and 7 yield

$$\frac{\partial u}{\partial z}+\frac{k_0}{\mu}\left(\begin{array}{c}-\frac{v}{r}\frac{\partial v}{\partial z}-\frac{\partial u}{\partial z}\frac{\partial w}{\partial z}+\frac{\partial u}{\partial z}\frac{\partial u}{\partial r}+\frac{\partial v}{\partial z}\frac{\partial v}{\partial r}\\ +\frac{\partial w}{\partial z}\frac{\partial w}{\partial r}-\frac{\partial u}{\partial r}\frac{\partial w}{\partial r}+u\frac{\partial^2 u}{\partial r\partial z}\\ +w\frac{\partial^2 u}{\partial z^2}+w\frac{\partial^2 w}{\partial r\partial z}+u\frac{\partial^2 w}{\partial r^2}\end{array}\right)=\frac{k}{\mu}\left(\frac{\pi}{Q}\right)^n u(ru)^n\left[u^2+(\omega r-v)^2\right]^{\frac{n-1}{2}}, \quad (13)$$

$$\frac{\partial v}{\partial z}+\frac{k_0}{\mu}\left(\begin{array}{c}\frac{u}{r}\frac{\partial v}{\partial z}-\frac{\partial v}{\partial z}\frac{\partial w}{\partial z}+w\frac{\partial^2 v}{\partial z^2}\\ +\frac{v}{r}\frac{\partial w}{\partial r}-\frac{\partial v}{\partial r}\frac{\partial w}{\partial r}+u\frac{\partial^2 v}{\partial r\partial z}\end{array}\right)=-\frac{k}{\mu}\left(\frac{\pi}{Q}\right)^n(\omega r-v)(ru)^n\left[u^2+(\omega r-v)^2\right]^{\frac{n-1}{2}}. \quad (14)$$

Furthermore, the continuity of the axial velocity components at the interface gives

$$w\left(r,\delta(r)\right)=W\left(r,\delta(r)\right)=0, \quad (15)$$

Assuming that the lubrication layer is very thin, boundary conditions (13), (14) and (15) can be imposed at the surface when $z=0$ as proposed by Andersson and Rousselet (2006).

The free stream boundary conditions are given by

$$u=0,\quad v=0. \quad (16)$$

To solve the system of partial differential equations obtained from Equation 3, the following dimensionless variables were introduced:

$$\eta=z\sqrt{\frac{\omega}{\nu}},\ u=\omega r f(\eta),\ v=\omega r g(\eta),\ w=\sqrt{\omega\nu}h(\eta),\ P=\omega\mu\, p(\eta) \quad (17)$$

The reduced system of coupled non-linear ordinary differential equations along with boundary conditions is

$$h'=-2f \quad (18)$$

$$f''-hf'-f^2+g^2+We\left(hf'''+4ff''+2g'^2\right)=0, \quad (19)$$

$$g''-hg'-2fg+We(hg'''+4fg''-2f'g')=0, \quad (20)$$

$$p'+2f'-2fh+We(12ff'+2f''h)=0. \quad (21)$$

$$h(0)=0\,,\ p(0)=0\,, \quad (22)$$

$$f'(0)+We[2f(0)f'(0)-f'(0)h'(0)+h(0)f''(0)]=\lambda(f(0))^{\frac{4}{3}}\left[(f(0))^2+(1-g(0))^2\right]^{-1/3} \quad (23)$$

$$g'(0)+We[2f(0)g'(0)-g'(0)h'(0)+h(0)g''(0)]=-\lambda(f(0))^{\frac{1}{3}}(1-g(0))\left[(f(0))^2+(1-g(0))^2\right]^{-1/3} \quad (24)$$

$$f(\infty)=0\,,\ g(\infty)=0 \quad (25)$$

where $We=k_0\omega/\rho\nu$ is the Weissenberg number and

$$\lambda=\frac{k\sqrt{\nu}}{\mu}\left(\frac{\pi}{Q}\right)^{\frac{1}{3}}\frac{\omega^{\frac{2}{3}}}{\omega^{\frac{5}{2}}}. \quad (26)$$

It is worth mentioning that we have used $n=1/3$ in Equations 23 and 24 in order to obtain similarity solution. From Equation 26, the constant λ can be written as

$$\lambda = \frac{\sqrt{\frac{\nu}{\omega}}}{\frac{\mu}{k}\left(\frac{Q\omega}{\pi}\right)^{\frac{1}{3}}} = \frac{L_{visc}}{L_{lub}}. \quad (27)$$

It is clear from Equation 27 that the parameter λ is the ratio of viscous length and lubrication length scales, respectively. When the lubricant is highly viscous and the lubrication length is small, λ becomes large. In the limiting case when $\lambda \to \infty$, the conventional no-slip conditions $f(0) = 0$ and $g(0) = 1$ are obtained from Equations 23 and 24. In the reverse case, when $\lambda \to 0$, one obtains the full-slip boundary conditions $f'(0) = 0$ and $g'(0) = 0.$ Hence, λ is known as slip parameter.

NUMERICAL RESULTS AND DISCUSSION

To analyze the behaviour of parameters λ and We on velocity and pressure profiles, the Equations 18 to 21 together with boundary conditions 22 to 25 are solved numerically by the Keller-Box method (Keller and Cebeci, 1972; Bradshaw et al., 1981; Keller, 1970).

Figures 2 to 6 are plotted to see the effects of slip parameter λ on velocity profiles f, g, h and pressure p for some fixed values of Weissenberg number, while the effects of We in the presence of slip are shown in Figures 6 to 10. Dashed lines shown in Figures 2 to 6 are the reproduced results already calculated by Andersson and Rousselet (2006) through Keller-Box method for the case of Newtonian fluid (that is, $We = 0$). Numerical computations for both the components of skin friction coefficients under the influence of pertinent parameters are presented in Tables 1 to 2.

Figure 2 is displayed to show the effects of slip parameter λ on axial velocity when $We = 1$. It is important to mention here that as the numerical values of λ is increased, an increase in the value of $-h$ is observed. Also, the thickness of boundary layer region is increased by increasing the numerical value of λ. Figure 3 shows the variation in the radial velocity f caused by the centrifugal force under the influence of slip parameter. It is clear from Figure 3 that by increasing slip on the surface, f decreases. The variation in radial velocity has the same behaviour as observed for the viscous fluid (dashed lines) except the peak value which was near 0.18 at $\eta = 0.90$ for the viscous fluid when there is no-slip (2006) and is now near 0.225 when η is about 1.1 (near unity) for the second grade fluid. The gradual increase in the radial velocity in Figure 3 with increasing value of λ is directly related with the distributions of the h-profile shown in Figure 2. This is due to the direct relation between f and h shown in Equation 18.

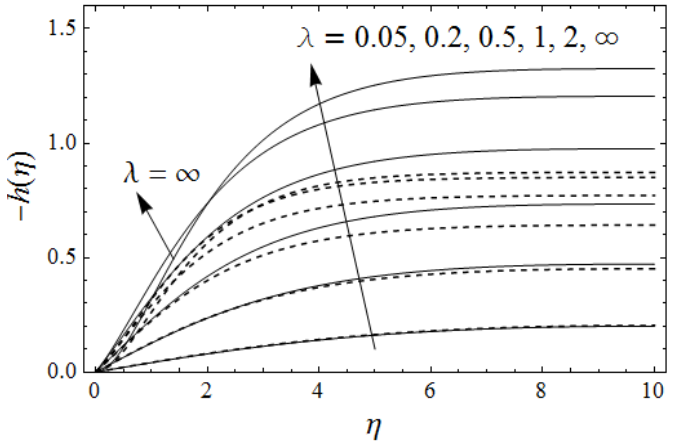

Figure 2. Variation of $-h(\eta)$ for different values of λ when $We = 1$. Dashed lines are calculated by Andersson and Rousselet (2006).

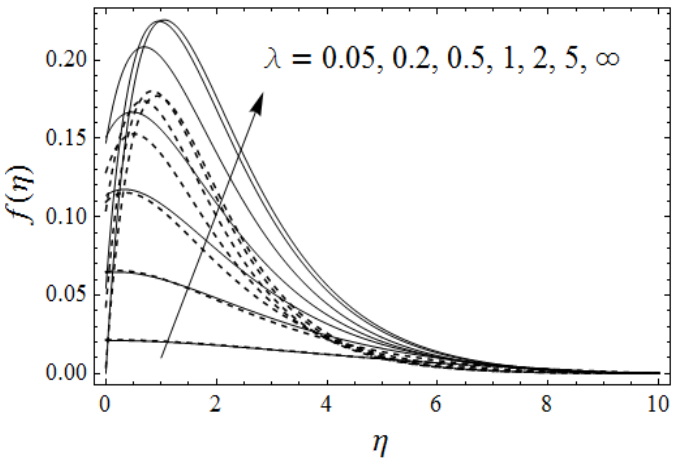

Figure 3. Variation of $f(\eta)$ for different values of λ when $We = 1$. Dashed lines are calculated by Andersson and Rousselet (2006).

Effect of slip parameter on the azimuthal velocity component g in the circumferential direction is depicted in Figure 4. It is obvious from Figure 4 that by increasing λ, the numerical value of g is increased. The torque required to maintain steady rotation of the disc is controlled by this component of the velocity. The imposed torque decreases monotonically by increasing slip on the surface. It is evident from Figures 2 to 4 that the variation in the three velocity components is more significant for smaller values of λ showing that power-law lubricant increases the fluid velocity at the surface.

The variation in the pressure under the influence of slip parameter when $We = 1$, is observed in Figures 5 and 6.

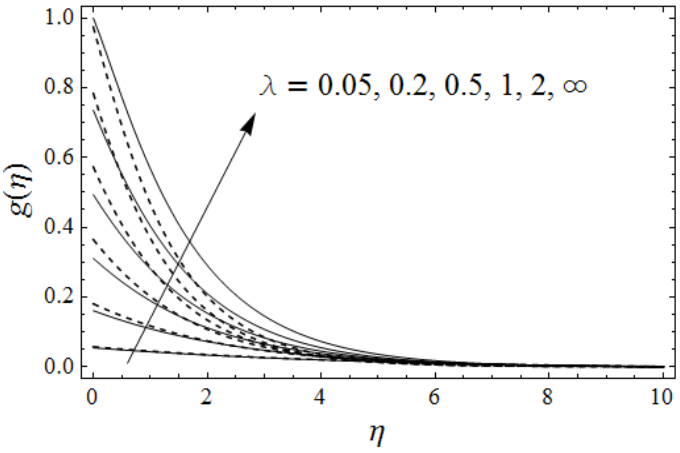

Figure 4. Variation of $g(\eta)$ for different values of λ when $We = 1$. Dashed lines are calculated by Andersson and Rousselet (2006).

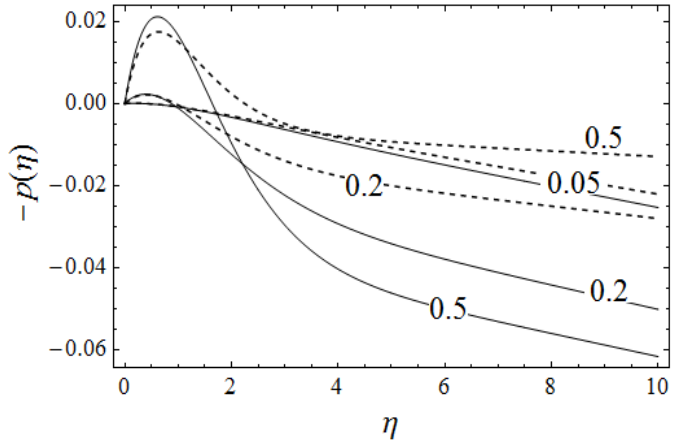

Figure 5. Effect of slip on pressure when $We = 1$.

It is clear from Figure 6 that pressure increases by decreasing slip. However, the behaviour of pressure distribution near the full slip is different as shown in the Figure 5. For $\lambda \leq 1$ the disc pressure is less than the ambient pressure $-p(\infty)$, which means that the flow is driven towards the disc by the axial pressure gradient in this particular range of λ.

Effect of We on h-profile when $\lambda = 1.5$ is shown in Figure 7. It is obvious from this figure that by increasing We, the axial velocity component is increased. The velocity profile shown by dashed line is for viscous fluid, that is, when $We = 0$. Figure 8 shows the variation in radial velocity component f when We ranges from 0 to 5 and $\lambda = 1.5$. It is evident from this figure that f

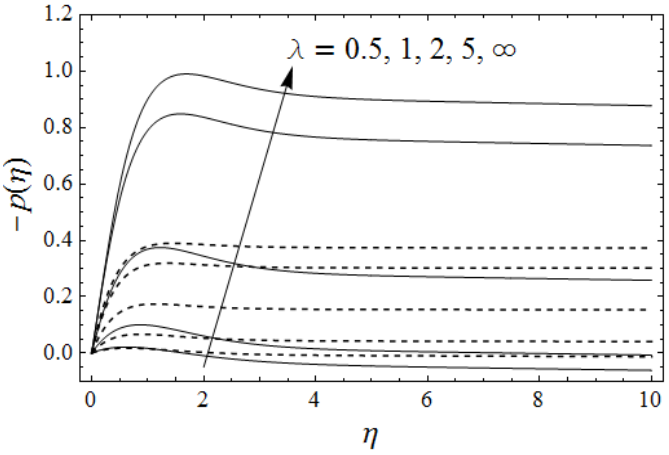

Figure 6. Effect of slip on pressure when $We = 1$.

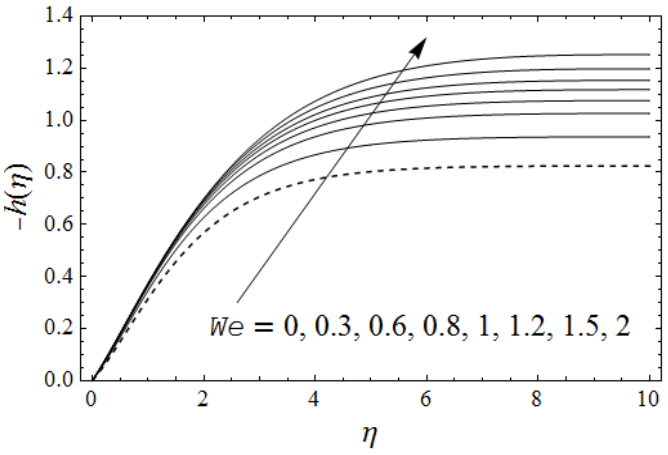

Figure 7. Variation of $-h(\eta)$ for different values of We when $\lambda = 1.5$.

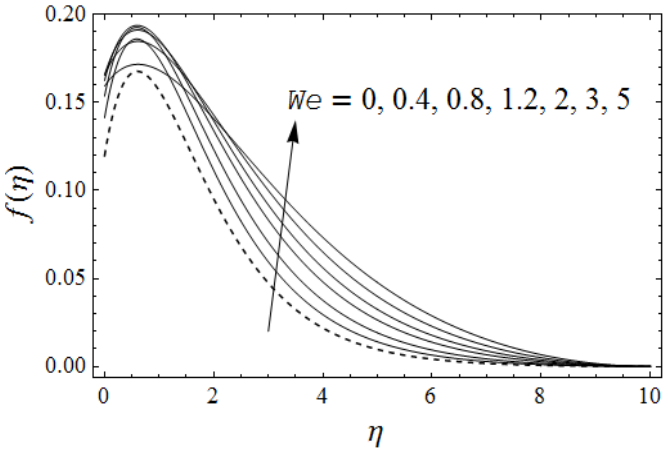

Figure 8. Variation of $f(\eta)$ for different values of We when $\lambda = 1.5$.

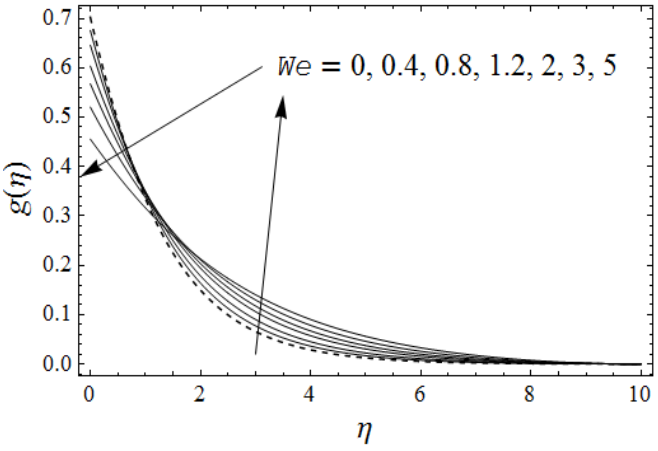

Figure 9. Variation of $g(\eta)$ for different values of We when $\lambda = 1.5$.

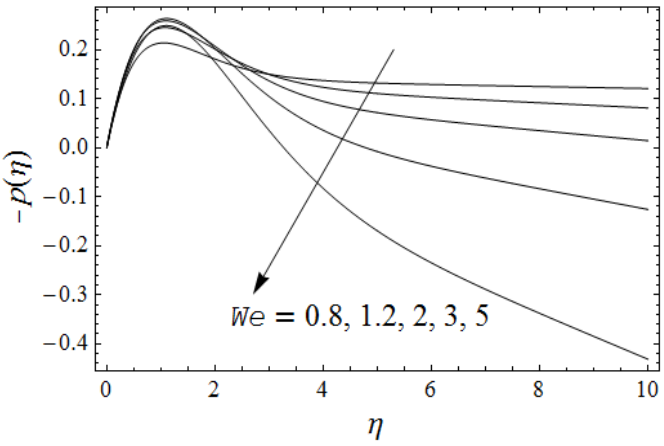

Figure 11. Variation of $-p(\eta)$ for different values of We when $\lambda = 1.5$.

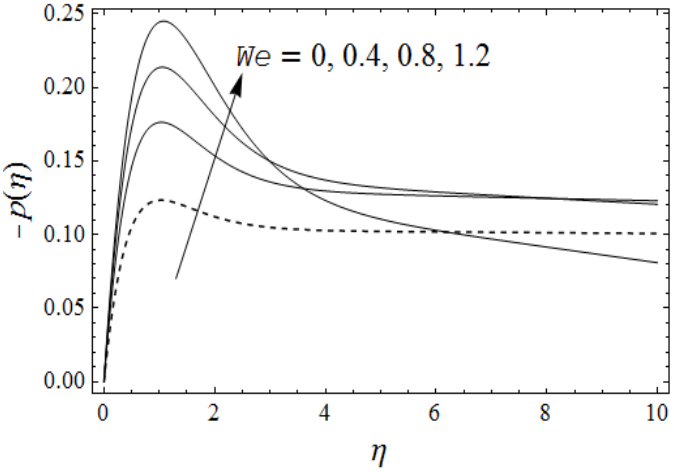

Figure 10. Variation of $-p(\eta)$ for different values of We when $\lambda = 1.5$.

increases with an increase in Weissenberg number. Some reverse effects was observed on the peak for higher values of We. The azimuthal velocity component g is presented in Figure 9. It is evident from this figure that g increases by increasing the value of We when λ is fixed. An opposite behaviour in the shear component of velocity is observed near the surface. Figures 10 and 11 are plotted for the pressure distribution using various values of We when $\lambda = 1.5$. It is clear from these figures that $-p$ increases when $0 \leq We < 0.8$. After this pressure profile shows an increase near the surface and then decreases dramatically.

Table 1 elucidates the change in numerical values of $f'(0)$ and $g'(0)$ for various values of λ when $We = 0.05$ and $We = 1$. It is clear from the Table 1 that as λ increases from 0 to ∞, the numerical values of $f'(0)$ increase. However, the numerical values of $g'(0)$ initially increase and then start decreasing. The numerical values of $f'(0)$ and $g'(0)$ for different values of We when $\lambda = 0.05$ and $\lambda = 1.5$ are presented in Table 2. According to this table as the numerical value of We increases, the numerical values of $f'(0)$ increase while those of $g'(0)$ decrease.

Conclusion

In this paper, the slip flow of a second grade fluid over a rotating disc lubricated with a thin layer of power-law fluid was examined. The governing equations along with boundary conditions are transformed to ordinary differential equations by a suitable choice of transformation. To obtain true similarity solutions, we selected $n = 1/3$. The numerical solutions were computed using Keller-Box method. The motivation is to determine the effects of the slip parameter λ and We on the flow characteristics. The cases of full slip for $\lambda \to 0$ and no slip for $\lambda \to \infty$ can be deduced from the present results. The main findings are investigated as under.

As the slip increases the numerical values of all the three components of velocity are decreased.

Numerical value of all velocity components is decreased as We is decreased.

An unexpected reversal in the pressure gradient has been observed for the lower values of λ and We.

Table 1. Numerical values of $f'(0)$ and $g'(0)$ for various values of λ.

$W_s = 0.05$			$W_s = 1$		
λ	$f'(0)$	$g'(0)$	λ	$f'(0)$	$g'(0)$
0.01	-0.000119	0.000056	0.01	-0.000119	0.000055
0.05	-0.002743	0.002407	0.05	-0.002556	0.002074
0.1	-0.008848	0.007804	0.1	-0.007839	0.006160
0.5	-0.119575	0.077270	0.5	-0.086636	0.043736
1.0	-0.311114	0.141201	1.0	-0.220373	0.068210
2.0	-0.614639	0.152593	2.0	-0.518510	0.029763
5.0	-0.908031	0.056128	5.0	-1.053342	-0.261694
10	-0.990542	0.004268	10	-1.232311	-0.406746
50	-1.032491	-0.028260	50	-1.320843	-0.484123
100	-1.035151	-0.030489	100	-1.326394	-0.489068
500	-1.036475	-0.031607	500	-1.329053	-0.491426
∞	-1.036605	-0.031717	∞	-1.329155	-0.491531

Table 2. Numerical values of $f'(0)$ and $g'(0)$ for various values of We.

$\lambda = 0.05$			$\lambda = 1.5$		
We	$f'(0)$	$g'(0)$	We	$f'(0)$	$g'(0)$
0	−0.002753	0.002427	0	−0.478938	0.168179
0.001	−0.002753	0.002427	0.001	−0.479043	0.168021
0.01	−0.002751	0.002423	0.005	−0.479498	0.167321
0.05	−0.002743	0.002407	0.01	−0.480046	0.166445
0.1	−0.002733	0.002388	0.05	−0.483640	0.159458
0.6	−0.002635	0.002206	0.1	−0.486222	0.150860
1.0	−0.002556	0.002074	0.5	−0.453483	0.096387
1.5	−0.002461	0.001925	1	−0.368705	0.062445
2	−0.002370	0.001791	1.5	−0.294832	0.046572
3	−0.002202	0.001565	2	−0.239556	0.037693
5	−0.001922	0.001230	3	−0.168367	0.027724
10	−0.001462	0.000766	5	−0.100475	0.018027

The computed results show that spin-up by second grade bulk fluid near the rotating disc is reduced by increasing slip. The radially directed centrifugal force is also reduced. The radial slip is turned out to be insufficient to outweigh the reduced centrifugal force.

The numerical values of $f'(0)$ increase as λ increases from 0 to ∞. However, the numerical values of $g'(0)$ initially increase and then start decreasing.

As Weissenberg number We increase, the numerical values of $f'(0)$ increase while those of $g'(0)$ decrease.

Conflict of Interests

The authors have not declared any conflict of interests.

Nomenclature

Q: Flow rate

P: Fluid pressure

δ: Thickness of lubrication layer

r, θ, z: Cylindrical coordinates

u, v, w: Velocity components of second grade fluid in radial, azimuthal and axial direction

ρ: Density

μ: Viscosity of second grade fluid

k_0: Material parameter

ω: Velocity of disc

λ: Slip parameter

μ_L: Viscosity of power- law fluid

U, V, W: Velocity components of Power-law fluid in radial, azimuthal and axial direction

n: Flow behavior index of Power-law fluid

We: Weissenberg number

k: Consistency coefficient of power-law fluid.

REFERENCES

Afrand M, Sina N, Teimouri H, Mazaheri A, Safaei MR, Esfe MH, Kamali J, Toghraie D (2015). Effect of Magnetic Field on Free Convection in Inclined Cylindrical Annulus Containing Molten Potassium. Int. J. Appl. Mech. 7(4):1550052.

Andersson HI, Rousselet M (2006). Slip flow over a lubricated rotating disc. Int. J. Heat Fluid Flow 27:329-335.

Ariel PD (1997). Computation of flow of a second grade fluid near a rotating disk. Int. J. Eng. Sci. 23:1335-1357.

Ariel PD (2002). On extra boundary condition in the stagnation point flow of a second grade fluid. Int. J. Eng. Sci. 40:145-162.

Asghar S, Hanif K, Hayat T, Khalique CM (2007). MHD non Newtonian flow due to non-coaxial rotations of an accelerated disk and a fluid at infinity. Commun. Nonlinear Sci. Num. Simulation 12:465-485.

Asghar S, Jalil M, Hussan M, Turkyilmazoglu M (2014). Lie group analysis of flow and heat transfer over a stretching rotating disk. Int. J. Heat Mass Transfer 69:140-146.

Attia HA (2009). Steady flow over a rotating disk in a porous medium with heat transfer. Nonlinear Anal. Model. Control 14:21-26.

Beard BW, Walters K (1964). Elastico-viscous boundary layer flows. I. Two-dimensional flow near a stagnation point. Proc. Cambridge Philosophical Soc. 60:667-674.

Benton ER (1966). On the flow due to a rotating disk. J. Fluid Mech. 24:781-800.

Bradshaw V, Cebeci T, Whitelaw IH (1981). Engineering Calculation Methods for Turbulent Flows. Academic, London.

Cochran WG (1934). The flow due to a rotating disc. Proc. Cambridge Philosophical Soc. 30:365-375.

Garg VK, Rajagopal KR (1990). stagnation point flow of a non-Newtonian fluid. Mech. Res. Commun. 17:415-421.

Hanna DM (1947). Forced flow against a rotating disc. British Aeronautical Research Council Reports and Memoranda, No. 2772, University of Michigan.

Kakutani T (1962). Hydromagnetic flow due to a rotating disk. J. Phys. Soc. Japan 17:1496-1506.

Keller HB (1970). A New Difference Scheme for Parabolic Problems, in Numerical Solution of Partial Differential Equations (J. Bramble, ed.). Volume II, Academic, New York.

Keller HB, Cebeci T (1972). Accurate Numerical Methods for Boundary Layer Flows II: Two Dimensional Turbulent Flows. Am. Inst. Aeronautics Astronautics 10:1193-1199.

Kumar SK, Thacker WI, Watson LT (1988). Magnetohydrodynamic flow past a porous rotating disk in a circular magnetic field. Int. J. Num. Methods Fluids 8:659-669.

Labropulu F, Li D (2008). Stagnation-point flow of a second grade fluid with slip. Int. J. Non-Linear Mech. 43:941-947.

Malvandi A, Safaei MR, Kaffash MH, Ganji DD (2015). MHD mixed convection in a vertical annulus filled with Al_2O_3-water nanofluid considering nanoparticle migration. J. Magnetism Magnetic Mater. 382:296-3069.

Miklavcic M, Wang CY (2004). The flow due to a rotating disk. J. Appl. Math. Phys. 54:1-12.

Pande GS (1971). On the effects of uniform high suction on the steady hydromagnetic flow due to a rotating disk. Appl. Sci. Res. 11:205-212.

Rajagopal KR, Gupta AS (1984). An exact solution for the flow of a non-Newtonian fluid past an infinite plate. Meccanica 19:158.

Safaei MR., Rahmanian B, Goodarzi M (2011). Numerical Study of Laminar Mixed Convection Heat Transfer of Power-Law Non-Newtonian Fluids in Square Enclosures by Finite Volume Method. Int. J. Phys. Sci. 6(33):7456-7470.

Santra B, Dandapat BS, Andersson HI (2007). Axisymmetric stagnation-point flow over a lubricated surface. Acta Mechanica 194:1-10.

Sparrow EM, Chess RD (1962). Magnetohydrodynamic flow and heat transfer about a rotating disk. ASME J. Appl. Mechanics 29:181-187.

Sparrow EM, Gregg JL (1960). Mass transfer, flow, and heat transfer about a rotating disk. ASME J. Heat Transfer 82:294-302.

Tifford AN, Chu ST (1952). On the flow around a rotating disc in a uniform stream. J. Aeronautical Sci. 19:284-285.

Turkyilmazoglu M (2009). Exact solutions for the incompressible viscous fluid of a porous rotating disk flow. Int. J. Non-Linear Mechanics 44(4):352-357.

Turkyilmazoglu M (2012a). An implicit spectral method for the numerical solution of unsteady flows with an application to rotating disk flow and heat transfer, Isi Bilimi Ve Teknigi Dergisi/. J. Thermal Sci. Technol. 32(2):99-106.

Turkyilmazoglu M (2012b). Three dimensional MHD stagnation flow due to a stretchable rotating disk. Int. J. Heat Mass Transfer 55(23-24):6959-6965

Turkyilmazoglu M (2014). MHD fluid flow and heat transfer due to a shrinking rotating disk. Comput. Fluids 90:51-56.

Turkyilmazoglu M (2015). Bödewadt flow and heat transfer over a stretching stationary disk. Int. J. Mech. Sci. 90:246-250.

Turkyilmazoglu M, Senel P (2013). Heat and mass transfer of the flow due to a rotating rough and porous disk. Int. J. Thermal Sci. 63:146-158.

Von KT (1921). Uberlaminare und turbulente Reibung. J. Appl. Math. Mech. 1:233-252.

Wang CY (2003). Stagnation flows with slip: Exact solution of the Navier-Stokes equations. Zeitschrift für Angewandte Mathematik und Phys. 54:184-189.

Wang CY (2008). Off-centered stagnation flow towards a rotating disc. Int. J. Eng. Sci. 46:391-396.

Watanabe T, Oyama T (1991). Magnetohydrodynamic boundary layer flow over a rotating disk, Zeitschrift fur Angewandte Mathematik und Mechanik 71:522-524.

Watson LT, Wang CY (1979). Deceleration of a rotating disk in a viscous fluid. Phys. Fluids 22:2267-2269.